Supplemental methods

PCR primers for genotyping

Wild-type gene: SART1 wt F/R (896 bp product in wild-type and heterozygous mice): GAAACGCGATGACGGCTACGAGG / CCTATGGGCAGACTGTGGGTTCC

LacZ disruption: V76 F/ SART1 wt R (het/ko yields product 578 bp – no product in wild-type mice) CTTGCAAAATGGCGTTACTTAAGC/ CCTATGGGCAGACTGTGGGTTCC

Cell lines and siRNA transfections. Huh7 human hepatoma cells and THP-1 human monocyte cells were purchased from Japanese Collection of Research Bioresources (JCRB, NIBIO Osaka, Japan) and American Type Culture Collection (ATCC, Manassas VA) respectively and verified by STR fingerprinting. Huh7 and THP-1 cells were transfected with siRNA using Lipofectamine 2000 (Invitrogen, Life Technologies, Grand Island NY) or Dharmafect 4 (GE Dharmacon Lafayette, CO) respectively according to the manufacturer's protocol. THP-1 cells were differentiated with 25ng/ml phorbol myristate acetate (PMA, Sigma –Aldrich, St. Louis MO) 24 hours prior to siRNA transfection. Both cell lines were transfected with siRNA 72 hours prior to assay. HAF (*SART1*) siRNA was ON-Targetplus SMARTpool (Dharmacon L-017283, siHAF or siHAF_1), and Hs_SART1_3 (siHAF_2, Qiagen, Germantown MD). Control siRNA (siCon) was siGENOME Non-targeting siRNA#3 (Dharmacon). All siRNAs were transfected at a final concentration of 40nM.

Western blotting (WB) and immunohistochemistry (IHC). HIF-1α/CD68 dual staining was performed using Chromoplex1 Dual detection (DS 9477, Leica Biosystems, Buffalo Grove IL). IHC for HIF-1α and HAF was performed as previously described (1). IHC antibodies for Ly6G,

Cd68 and RANTES were from BD Pharmingen (#559286 BD Biosciences San Jose CA), Novus Biologicals (NB 100-2086 Littleton, CO) and Abcam (#ab9679, Cambridge, MA) respectively, whereas HIF-1α and HIF-2α antibodies used in mouse tissue were from Novus (NB100-479, NB100-122). WB was performed using Acsl1, Cyp2b10, actin and HAF from Cell signaling Technology (4047S, Danvers MA), EMD Millipore (AB9916), Santa Cruz Biotechnology Inc. (I-19, Dallas, TX), or made-in house respectively (2) .

Quantitation of blots in **Fig. 1D** was performed by normalizing HAF to its respective actin, and then normalizing this ratio to that of the same organ in the wild-type on the same blot. This was done for 4 pairs of mice and then averaged.

Gene expression analysis. Hit validation was performed by Taqman custom arrays (Life Technologies, Carlsbad CA) according to the manufacturer's protocol using the following pre-designed primer/probe sets:

B2m-Mm00437762_m1; Srebf1-Mm00550338_m1; Pparg-Mm01184322_m1; Mlxipl-Mm02342723_m1; Ppara-Mm00440939_m1; Acox1-Mm01246831_m1; Acsl1-Mm00484217_m1; Acaa1a-Mm00728460_s1; Pkm-Mm00834102_gH, Hk1-Mm00439344_m1 Slc2a1-Mm00441480_m1; Ccl5-Mm01302427_m1; Sart1-Mm00600274_m1.

All measurements were performed in duplicate per mouse with at least 2 mice/group (wild-type and *SART1*$^{+/-}$) for each age group. Data were normalized using β_2-microglobulin (B_2M) as the internal reference by the $\Delta\Delta$-C_T method (3) and GeneAmp 5700 SDS software (Life Technologies).

Kupffer cell (KC) isolation and cytokine analysis. KCs were isolated using *in vitro* collagenase incubation following liver perfusion as previously described (4). After Percoll purification and RBC lysis, cells were washed twice in RPMI 1640 media (Life Technologies) containing 10% FBS, and seeded at a density of 10^6 cells in 6-well plates. After washing to remove non-adherent cells, cells were left to recover for 24-36 hours, after which media was changed for an additional 6 hours. Media was then removed for cytokine analysis using the Mouse Cytokine Array C3 (Raybiotech Inc, Norcross GA) according to manufacturer's protocol. Films were scanned using the CanoScan 9000 scanner and quantitated by Raybiotech using in-house analysis software.

Seahorse Metabolic analysis. Hepatocytes were isolated using proprietary Liver Perfusion and Liver Digest Medium (Life Technologies) according to the manufacturer's protocol. Purified hepatocytes were seeded at 8000 cells/well in XF96 cell culture microplates (Seahorse Bioscience, MA) pre-coated with rat tail Collagen I (12.5µg/cm^2, Geltrex), starved overnight, then run on the XF^e96 extracellular flux analyzer the next day according to the manufacturer protocol. Huh7 cells (from JCRB, confirmed by STR fingerprinting), were reverse transfected with HAF or non-targeting siRNA (L-017283-00-0005, D-001210-05-20; GE Dharmacon, Lafayette CO) using Dharmafect 4 and seeded at 6500 cells/well in an XF96 cell culture microplate. OCR analysis was performed 72 hours after siRNA transfection.

Isolation of mononuclear cells. PBMCs and spleen mononuclear cells were prepared by standard protocols (5). For induction of HIF-1α, spleen cells were seeded at 4E6 cells/well 6-

well plates and exposed to hypoxia (1%O_2. 5% CO_2, InVivo$_2$ 400, Baker Ruskinn Sanford ME) for 2 hours prior to lysis. PBMCs were lysed immediately after purification.

Flow cytometry. Cells were washed in FACS buffer (2% FBS in PBS), stained for 30 minutes on ice, then washed twice in FACS buffer, and analyzed on the FACSCanto (BD Biosciences, San Jose CA) flow cytometer using 488 nm and 633 nm excitation. Antibodies used were from Ebiosciences as below:

Mouse liver profiling: Ly6G-FITC, CD11c-PE, CD3-APC, TCRgd-PE Cy7, CD45-Pacific Blue, CD19 Alexa fluor700;

Spleen profiling: TCRβ-PECy7, CD19-PE, F4/80-APC,Ly6G-APC Cy7, TCRγδ-PE, CD11c-APC, 7AAD-APCefluor780.

LacZ activity was quantitated using the Fluoreporter LacZ kit (Life Technologies F-1930) according to manufacturer's protocol.

MRI procedures. During the MRI procedures, anesthesia was maintained using a 1-2% isoflurane-in-oxygen mixture. Body temperature was maintained using a thermally regulated water heating blanket. After standard MRI preparation (optimization of shimming, pulse power calibration, scout images to locate the tumor), a respiratory-gated, T2-weighted, rapid acquisition with relaxation enhancement (RARE) sequence was acquired with repetition time=2.2s, echo-time=30ms, and 4 averages. A 25x35mm field of view with a 125x175 matrix was used with 24, contiguous 1.25mm-thick, transaxial slices that covered the entire liver tumor volume. Images

were analyzed using Amira 5.5.0. Individual tumor nodules were discerned based on their separation in 3D space from neighboring tumor nodules. All tumor growth in the liver was manually segmented on each slice in which tumor growth was resolved using the Amira Segmentation Editor. The presence of hepatic tumor nodules was confirmed grossly at necropsy, which was performed 48 hours after imaging, and by histopathologic examination of H&E stained sections.

References

1. Koh MY, Nguyen V, Lemos R, Darnay BG, Kiriakova G, Abdelmelek M, Ho TH, et al. Hypoxia-Induced SUMOylation of E3 Ligase HAF Determines Specific Activation of HIF2 in Clear-Cell Renal Cell Carcinoma. Cancer Research 2015;75:316-329.
2. Koh MY, Darnay BG, Powis G. Hypoxia-associated factor, a novel E3-ubiquitin ligase, binds and ubiquitinates hypoxia-inducible factor 1alpha, leading to its oxygen-independent degradation. Mol Cell Biol 2008;28:7081-7095.
3. Livak KJ, Schmittgen TD. Analysis of relative gene expression data using real-time quantitative PCR and the 2^{-DDCT} method. Methods 2001;25:402-408.
4. Kinoshita M, Uchida T, Sato A, Nakashima M, Nakashima H, Shono S, Habu Y, et al. Characterization of two F4/80-positive Kupffer cell subsets by their function and phenotype in mice. Journal of Hepatology 2010;53:903-910.
5. Kruisbeek AM: Isolation of Mouse Mononuclear Cells. In: Current Protocols in Immunology: John Wiley & Sons, Inc., 2001.

Supplemental figure legends:

S1: A) Terminal body weight of male wild-type and *SART1*$^{+/-}$ mice upon necropsy at age 14-18 months. B) MRI images of axial sections of live 16-18 month old *SART1*$^{+/-}$ male mice showing the presence of liver tumors. Dotted white circles indicate tumors and estimated volumes calculated from MRI slices are shown below images. Images of livers harvested from mice imaged are shown below MRI scans. C) MRI monitoring of tumor growth of mouse H1059 at

fortnightly intervals following MRI start with necropsied liver at end of study on RHS. Scale bar = 1cm. D) Age-related levels of blood serum liver enzymes ALT, AST, and ALP in circulating blood of male *SART1*$^{+/-}$ mice versus wild-type littermates (5 per group; mean ± SE). E) Table showing summary of age-related liver phenotypes in male wild-type and *SART1*$^{+/-}$ mice as verified by histology.

S2: Top biological functions identified using Ingenuity Pathway Analysis (IPA) of microarray data of RNA from *SART1*$^{+/-}$ liver tumor compared to wild-type liver from an age-matched wild-type mouse.

S3: A) Fold change in genes involved in fatty acid metabolism (according to IPA) from microarray data of RNA from *SART1*$^{+/-}$ liver tumor compared to wild-type liver from age-matched wild-type mouse. B) Fold change in a panel of secreted cytokines from Kupffer cells isolated from 5 month old male *SART1*$^{+/-}$ livers compared to those from age-matched wild-type livers as determined by intensity quantitation of ELISA membrane arrays (pooled from 4 mice per group).

S4: A) Western blot and quantitation of HIF-1α immunoprecipitated from homogenized liver sections from mice of indicated ages (normalized to non-specific band, NS). B) Western blot and quantitation of HIF-1α normalized to actin in isolated hepatocytes from 6 month old male wild-type and *SART1*$^{+/-}$ mice. C) Immunohistochemistry for HIF-2α in the livers of 12-month old

male wild-type and *SART1*$^{+/-}$ mice. Arrows indicate HIF-2α positive immune infiltrating cells. D) Western blot and quantitation of HAF levels in peripheral blood mononuclear cells (PBMCs), adherent and non-adherent spleen mononuclear cells isolated from 6 month old male *SART1*$^{+/-}$ and wild-type mice.

S5: Western blot and quantitation of HIF-1α levels (A), and HAF levels (B) in peripheral blood mononuclear cells (PBMCs), adherent and non-adherent spleen mononuclear cells isolated from 6 month old female *SART1*$^{+/-}$ and wild-type mice. C) Quantitation of levels of secreted cytokines from *SART1*$^{+/-}$ Kupffer cells (KCs) isolated from 6 month old female *SART1*$^{+/-}$ livers normalized to wild-type with ELISAs depicted inset (pooled from 3 mice/group).

S6: A) Flow cytometry scatterplots showing LacZ expression within different leukocyte cell populations isolated from spleen, peripheral blood, and bone marrow of male *SART1*$^{+/-}$ and wild-type mice (aged 4 months). Scatterplot key: All single cells (red/blue), live single cells (maroon), Lac Z positive (green).B) Representative scatterplots showing flow cytometry gating procedure for quantitation of CD19+/TCR β- (B-cells), CD19-/TCRβ+ (T-cells) and CD19-/TCRβ- (non-lymphocytes) , which were further resolved into populations defined by F4/80Hi/ Ly6- , F4/80HI/ Ly6MID, F4/80HI/Ly6HI, and F4/80-/Ly6HI. Histograms indicate LacZ positivity in each of the cell populations depicted with equivalent plots from a wild-type mouse shown in dark red. Results were from spleen of a 4 month-old mouse male *SART1*$^{+/-}$ *or* wild–type mouse.

S7: Scatterplots showing flow cytometry gating procedure for identification of Ly6G+ neutrophils in mouse livers and spleens (plots from 1 month-old mouse depicted).

S8: Pre-treatment axial MRI liver slices of male *SART1*$^{+/-}$ mice aged 16-18 months showing additional tumor nodules (white arrows) not visible in slices shown in **Fig. 7A**.

Supplemental data S1

A)

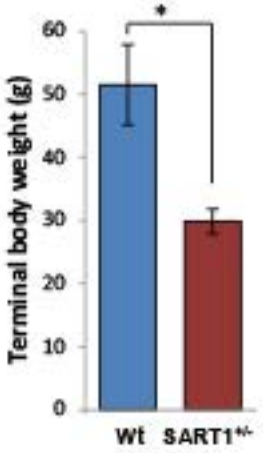

B)

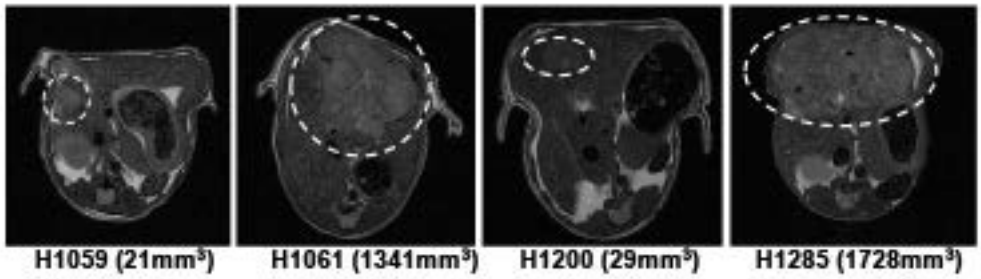

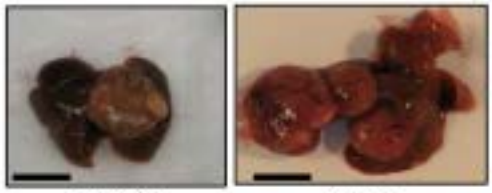

C)

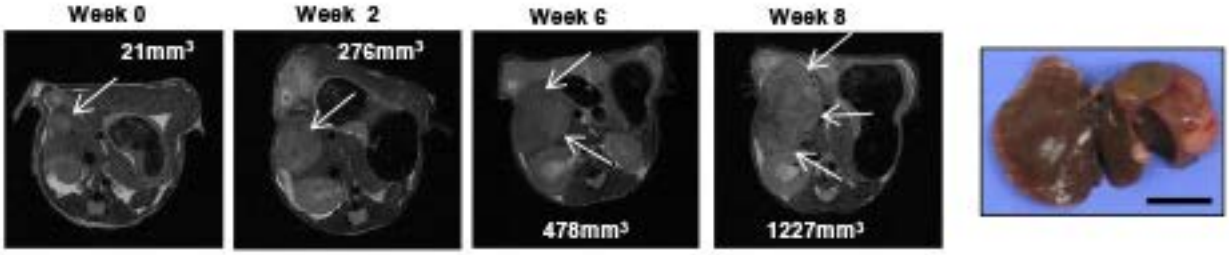

D)

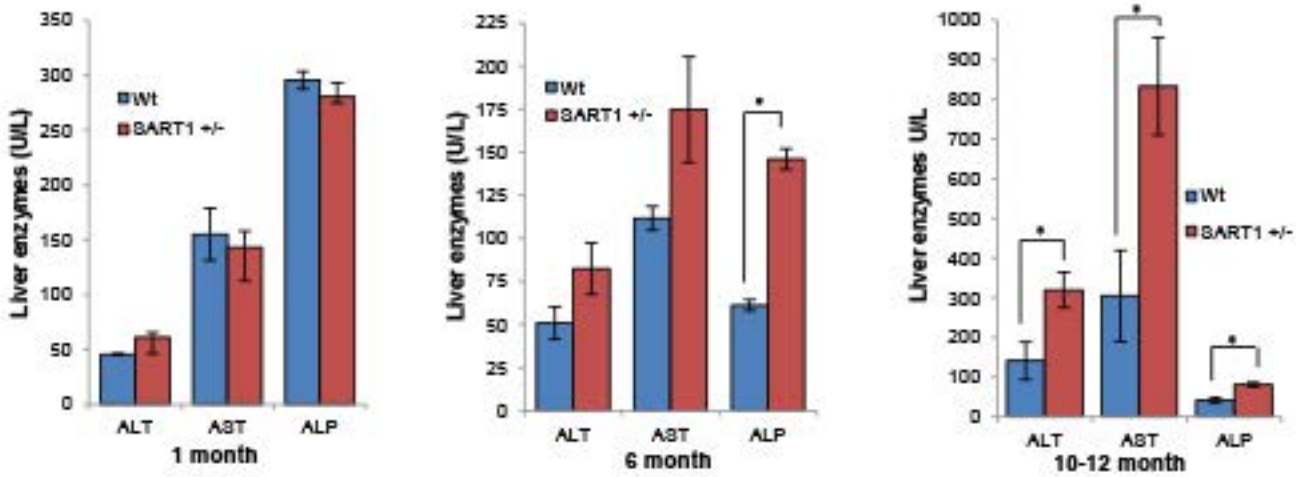

E)

Incidence/total

	1 month		6 months		10-12 months		14-18months	
Phenotype	Wild type	SART1+/-	Wild type	SART1+/-	Wild type	SART1+/-	Wild type	SART1+/-
Hepatic Steatosis	0/4	0/4	0/6	6/6	5/6	10/12	4/6	6/6
Focal nodular hyperplasia	0/4	0/4	0/6	0/6	0/6	3/12	0/6	5/6
Cellular alteration	0/4	0/4	0/6	6/6	0/6	10/12	0/6	4/6
HCC	0/4	0/4	0/6	0/6	0/6	5/12	0/6	5/6
Kupffer cell hyperplasia	0/4	0/4	0/6	0/6	0/6	7/12	0/6	6/6

A)

Probeset ID	Gene Symbol	Gene Title	RefSeq Transcript ID	p-value(T vs. N)	Fold-Change(T vs. N)
1416645_a_at	Afp	alpha fetoprotein	NM_007423	1.00353E-08	441.666
1416646_at	Afp	alpha fetoprotein	NM_007423	1.98063E-07	74.2429
1436879_x_at	Afp	alpha fetoprotein	NM_007423	2.41278E-08	90.9532

B)

Top biological functions	**p-value**	**# of molecules**
Diseases and disorders		
Inflammatory response	8.58E-21 - 1.51E-04	467
Cancer	2.83E-20 - 1.48E-04	1163
Molecular and Cellular Functions		
Cell death and survival	7.65E-16 - 1.47E-04	718
Lipid metabolism	1.92E-15 - 1.20E-04	403
Physiological System Development/Function		
Immune cell trafficking	6.62E-14 - 1.51E-04	302
Hepatotoxicity		
Liver Hyperplasia/Hyperproliferation	1.42E-12 - 6.09E-01	138
Liver Steatosis	4.10E-09 - 4.65E-01	70
Hepatocellular Carcinoma	4.37E-09 - 6.09E-01	99
Liver Proliferation	7.80E-08 - 4.96E-01	56
Liver Necrosis/Cell Death	2.62E-07 - 5.43E-01	67

Supplemental data S3

A)

Symbol	Fold Change
ACAA1	-2.030
ACAD10	-2.274
ACADSB	-3.893
ACAT1	-2.178
ACSL1	-6.348
ACSL4	2.999
ADH4	-7.695
ADH5	-2.089
ADHFE1	-4.116
AKR1D1	-2.197
ALDH2	-2.245
ALDH1A1	-2.383
Aldh1a7	-2.528
ALDH1B1	3.607
ALDH5A1	-2.512
ALDH7A1	-2.516
CYP1A1	7.702
CYP2B6	-37.690
Cyp2b13/Cyp2b9	3.297
CYP2C8	-17.770
CYP2C9	-3.274
CYP2C18	-118.904
Cyp2c44	-16.343
Cyp2c70	-2.398
Cyp2c40	-2.968
CYP2D6	-2.139
Cyp2d13	-6.310
CYP2E1	-5.786
CYP2J2	2.183
Cyp2j5	-14.008
Cyp2j9	-2.649
CYP3A5	-2.688
CYP4A11	-19.197
Cyp4a14	-60.819
CYP4A22	-3.674
CYP4F8	-2.803
CYP4F12	-11.376
ECH1	-2.096
GCDH	-4.279
HSD17B10	-3.211
IVD	-2.178
SDS	-2.020
SLC27A5	-3.888
SRD5A1	-6.201
SRD5A2	2.013

B)

	Wt	SART1+/-	Ratio
axl	0.00	101.08	NA
BLC	452.90	1,032.89	2.28
CD30L	0.00	40.34	NA
CD30/TNFRSF8	1,766.20	4,142.22	2.35
CD40	14.52	139.67	9.62
CRG-2	112.54	202.03	1.80
CTACK	715.63	1,718.56	2.40
CXCL16	2,030.75	11,092.12	5.46
Eotaxin	0.00	207.19	NA
Eotaxin-2	0.00	217.05	NA
FAS ligand	0.00	205.69	NA
Fractalkine	102.58	270.88	2.64
G-CSF	0.00	320.47	NA
GM-CSF	0.00	146.07	NA
IFN-gamma	38.65	167.78	4.34
IGF-BP-3	1,940.35	3,345.08	1.72
IGF-BP-5	562.38	1,232.84	2.19
IGF-BP-6	175.34	288.95	1.65
IL1-alpha	923.99	2,657.69	2.88
IL1-beta	0.00	102.88	NA
IL2	0.00	265.60	NA
IL3	8.21	21.21	2.58
IL3 Rb	0.00	204.97	NA
IL4	494.49	1,113.48	2.25
IL5	0.00	142.47	NA
IL6	10,050.78	13,934.42	1.39
IL9	197.33	547.60	2.77
IL10	179.99	438.96	2.44
IL12-p40/p70	0.00	1,636.97	NA
IL12-p70	1,733.16	3,164.66	1.83
IL13	103.79	327.93	3.16
IL17	0.00	89.08	NA
KC/CXCL1	211.43	2,684.04	12.69
Leptin R	0.00	105.63	NA
Leptin	944.18	3,185.11	3.37
LIX	7,974.30	13,809.82	1.73
L-Selectin	0.00	269.76	NA
Lymphotactin	551.68	986.39	1.79
MCP-1	13,762.20	18,624.97	1.35
MCP-5	221.39	729.07	3.29
M-CSF	2,772.96	3,796.18	1.37
MIG	235.13	411.05	1.75
MIP-1-alpha	221.83	398.03	1.79
MIP-1-gamma	10,542.12	35,829.82	3.40
MIP-2	1,405.39	6,200.02	4.41
MIP-3-beta	360.20	912.23	2.53
MIP-3-alpha	521.89	1,933.98	3.71
PF4	821.30	2,649.69	3.23
P-Selectin	2,517.78	6,127.50	2.43
RANTES/CCL6	**62.82**	**8,438.43**	**134.34**
SCF	0.00	486.86	NA
SDF-1-alpha	765.46	1,260.42	1.65
TARC	305.88	599.24	1.96
TCA-3	1,131.77	1,636.60	1.45
TECK	38.64	139.25	3.60
TIMP-1	3,305.63	3,799.94	1.15
TNF-alpha	0.00	125.72	NA
sTNF RI	332.36	4,782.19	14.39
sTNF RII	535.84	2,636.19	4.92
TPO	155.11	448.46	2.89
VCAM-1	0.00	142.80	NA
VEGF	0.00	409.19	NA

Supplemental data S4

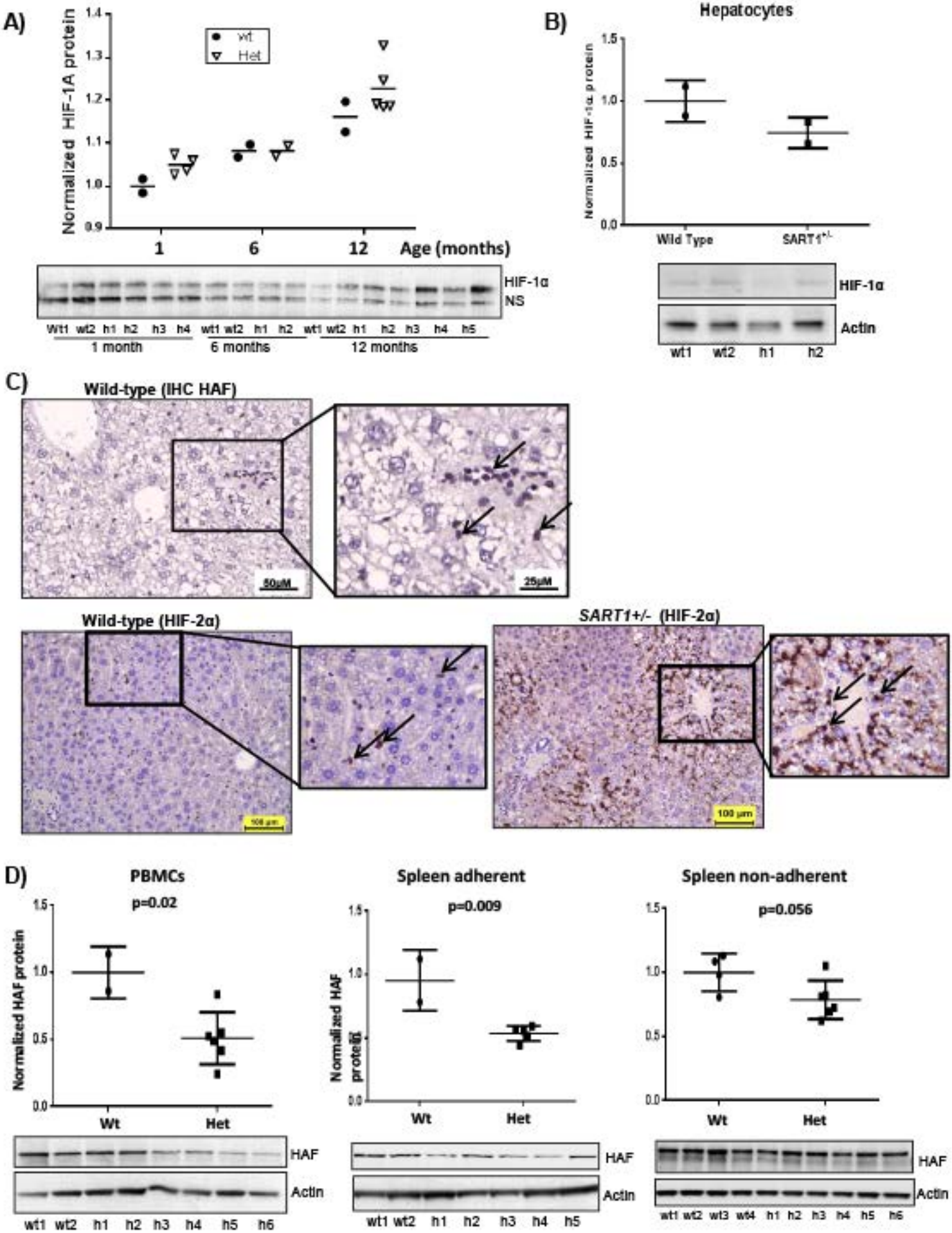

Supplemental data S5

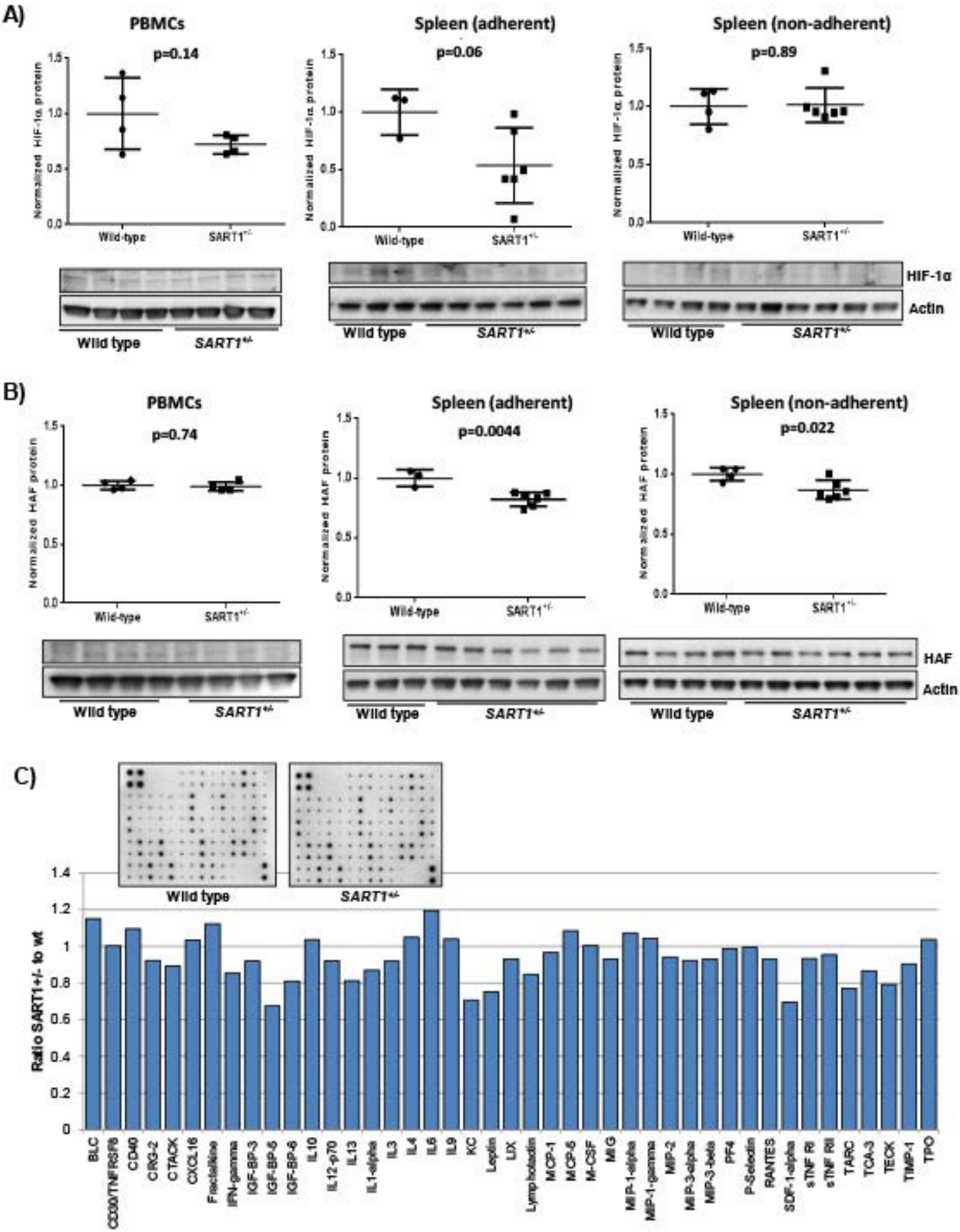

Supplemental data S6

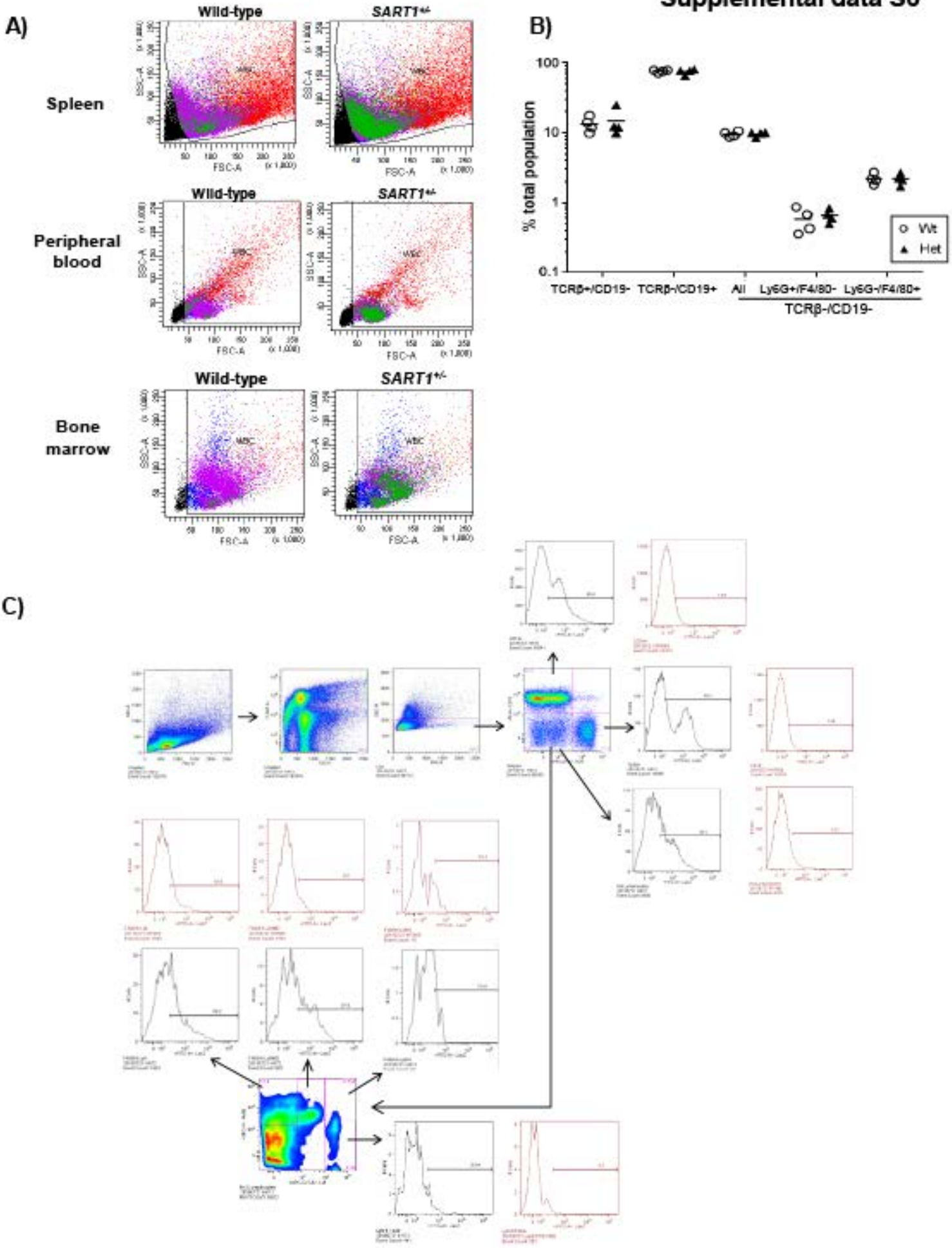

Supplemental data S7

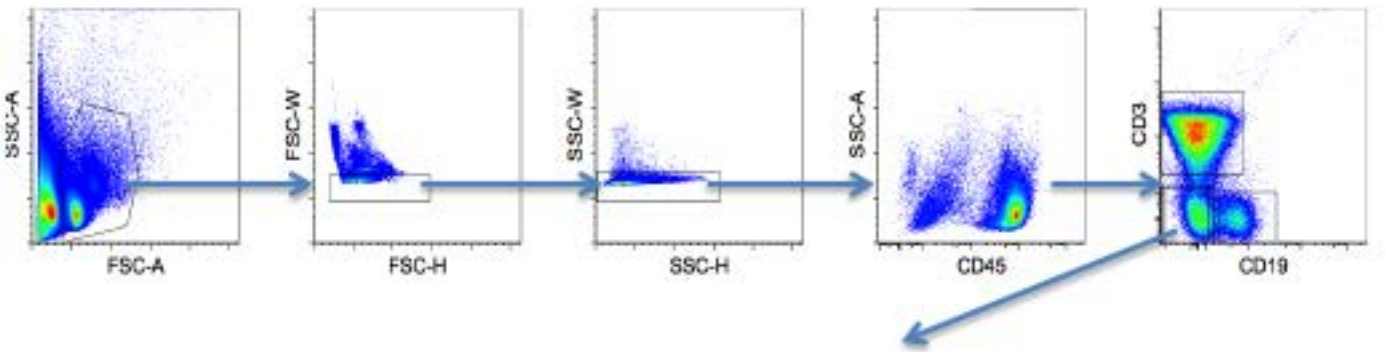

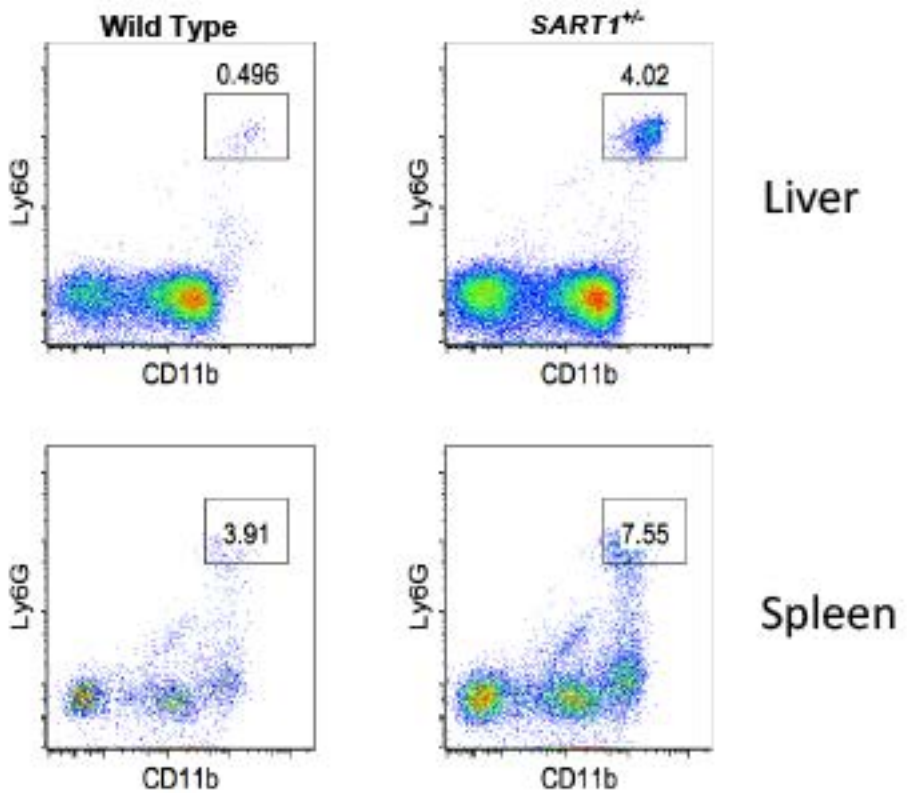

Pre-treatment MRI

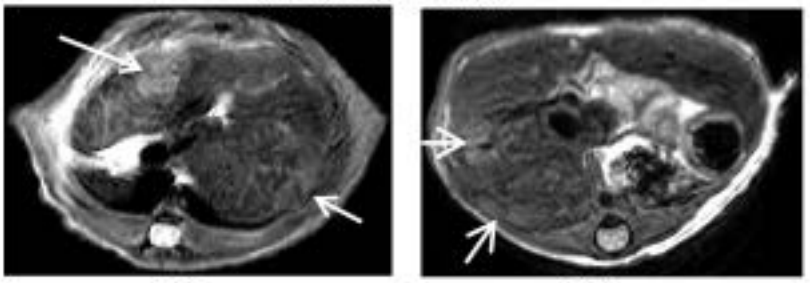

102 **277**